Accepted at the 2017 5th IEEE Global Conference on Signal and Information Processing (GlobalSIP).

INCORPORATING TIME-OF-DAY USAGE PATTERNS INTO NON-INTRUSIVE LOAD MONITORING

Chinthaka Dinesh, Stephen Makonin, and Ivan V. Bajić

School of Engineering Science, Simon Fraser University, Burnaby, BC, Canada
Email: hchintha@sfu.ca, smakonin@sfu.ca, ibajic@ensc.sfu.ca

ABSTRACT

Understanding appliance power consumption can help occupants optimize their power consumption behaviour. One popular class of methods for determining appliance power consumption is known as non-intrusive load monitoring (NILM). This paper shows how to incorporate time-of-day appliance usage patterns into a recent NILM method, resulting in both improved accuracy and reduction in computational complexity.

Index Terms— non-intrusive load monitoring (NILM), time-of-day usage, smart grid, load disaggregation, graph spectral representation

1. INTRODUCTION

Load monitoring techniques determine the appliances that are turned ON within a given period of time in a household or workplace [1]. They play a critical role in a variety of smart grid applications such as supply and demand side power control, adaptive billing, and appliance fault identification. Load monitoring is broadly classified as intrusive or non-intrusive. Intrusive load monitoring requires the attachment of individual sensors to each appliance being monitored, thus resulting in large initial expenses. However, in non-intrusive load monitoring (NILM), the objective is to determine which appliances are ON and their respective power consumptions through a single supply entry point [1], such as a smart meter. Thus, with its cost effectiveness and application potential for smart grids, there has been an escalation in the need for efficient and effective NILM methods for residential appliance identification [2–7]. Privacy is also an important concern for NILM. Although not the focus of this paper, these issues have been addressed in previous work [8].

Even though there are many diverse NILM methods proposed in the literature, most of them estimate the currently turned ON set of appliances only using electrical measurements such as current and/or voltage [9–12], active power [4–7, 13, 14], and reactive power [15]. However, certain appliances have a higher chance of being used at certain times of day. For example, a toaster would often get used in the morning, and likely never overnight. Very limited attention has been paid to utilizing such appliance usage patterns to develop more accurate NILM methods.

In this paper, the recent NILM method from [4] is extended to utilize time-of-day usage patterns of appliances. We use graph spectral representation to efficiently estimate joint time-of-day probabilities for sets of appliances. Incorporating this information into [4] leads to both improvement in NILM accuracy as well as reduction in complexity.

This work was funded in part by IC-IMPACTS.

2. METHODOLOGY

To simplify algorithm formulation, multi-state appliances are decomposed into multiple two-state (ON/OFF) appliances. Hereafter, when we refer to an "appliance," we mean a two-state (ON/OFF) appliance, whether it is originally a two-state appliance, or converted from a multi-state appliance.

2.1. Time-of-Day Usage Patterns

The proposed NILM method uses three types of features: spectral features, mean power levels, and time-of-day probabilities. The spectral features and mean power levels were generated using a Karhunen-Loeve Expansion (KLE)-based method described in [4]. Hence, we focus here on describing the time-of-day probabilities.

Certain appliances have a higher chance of being used at certain times of day. To capture such time-of-day usage patterns, we compute a time-of-day ON-probability for a set of appliances S as follows:

$$P[I_S(t) = 1] = \frac{n_S(t)}{N}, \tag{1}$$

where t is a certain time of day, N is the number of days in the training set, and $n_S(t)$ is the number of days in the training set in which all appliances in S were turned ON at time t. Here, S could be a single appliance ($S = \{a_i\}$), a pair of appliances ($S = \{a_i, a_j\}$), or a larger group of appliances ($S = \{a_{i_1}, a_{i_2}, ..., a_{i_n}\}$). However, since the total number of possible sets of appliances is large, we only pre-compute time-of-day probabilities for individual appliances and pairs of appliances. For sets of three or more appliances, we introduce an efficient method to estimate the corresponding joint probabilities in Section 2.2.

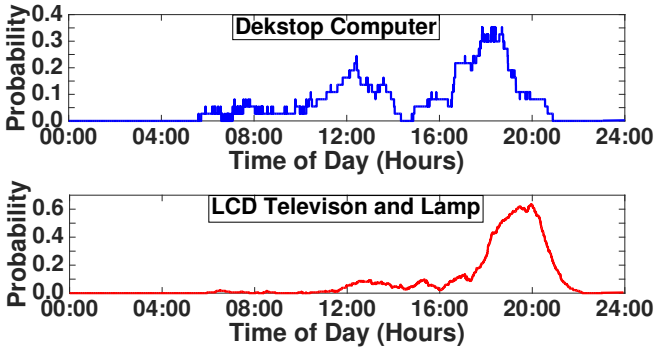

Fig. 1. Examples of time of day probabilities.

Fig. 1 shows time-of-day ON-probability for a desktop computer and the pair of appliances (LCD television, lamp). As seen in the figures, the probability of being ON clearly depends on the time of day. One could also appreciate that as the daylight time varies through the seasons, the lamp would be used at different times of day, depending on the season. This sort of information will be utilized to improve the NILM method from [4]. Here, we assume that there is a mechanism to collect a sufficient number of days of individual appliance power profiles in a given house in order to obtain reasonably accurate time-of-day usage patterns.

2.2. Appliance State Identification

In the NILM method of [4], the aggregate power signal is partitioned into non-overlapping windows called observation windows (OWs). For each OW, five principal components are extracted using KLE. Algorithm 1 presents the main steps for a given OW. Up to five iterations are executed, one for each principal component. In each iteration, two elimination steps are conducted, where each step removes some of the candidate sets of appliances. This is followed by the Maximum a Posteriori (MAP) estimation of the most likely set of appliances (S_{MAP}) that is turned ON in that OW.

Let Z_i be the event that the first i principal components are those observed in the first i iterations in a given OW. The goal of MAP estimation is to find the most likely set of appliances S that could have led to such an event. The Bayes' rule states that

$$P[I_S(t) = 1|Z_i] = \frac{P[Z_i|I_S(t) = 1] \cdot P[I_S(t) = 1]}{P[Z_i]}. \quad (2)$$

Here, t refers to the mid-point of the given OW. In [4], $P[Z_i|I_S(t) = 1]$ was determined for the non-eliminated sets in the last elimination step, just before the MAP estimation. With $S_{\text{MAP}} = \arg\max P[I_S(t) = 1|Z_i]$, if $P[I_{S_{\text{MAP}}}(t) = 1|Z_i] > 0.99$, the execution stops at the i-th iteration, before reaching the maximum of five iterations. The value 0.99 is the default threshold for the posterior probability in [4] and can be changed depending on the application. We kept the same threshold in this work.

If there are n appliances in a household, there are $2^n - 1$ sets of appliances to be considered, excluding the empty set.

Algorithm 1 Appliance identification algorithm from [4]

```
Set i = 1
Set execution = 1
Apply the pre-elimination step to the observation window;
while execution do
    Take the i-th principal component;
    Apply the two elimination steps;
    Conduct MAP estimation, find S_MAP;
    if P[I_{S_MAP}(t) = 1|Z_i] > 0.99 OR i == 5 then
        Output: S_MAP;
        Set execution = 0;
    else
        i = i + 1
    end if
end while
```

Due to the large number of sets, in [4], $P[I_S(t) = 1]$ was assumed to be equally likely for any set S. However, we know that this is not true in practice. Hence, we extend the method in [4] by computing the joint probabilities $P[I_S(t) = 1]$ with the help of graph spectral representation.

First, note that in the MAP estimation step, we only need to consider appliances sets S that have not been eliminated prior to the MAP step. Let us denote this set as $\mathcal{F} = \{S_1, S_2, ..., S_{n_S}\}$. In our experiments, n_S is usually less than 3% of the total number of possible sets.

The term $P[Z_i]$ in the denominator in (2) is common to all $S \in \mathcal{F}$, so removing it won't affect the maximization. Finally, the MAP problem becomes finding the set S that maximizes

$$P[I_S(t) = 1|Z_i] = P[Z_i|I_S(t) = 1] \cdot P[I_S(t) = 1]. \quad (3)$$

The term $P[Z_i|I_S(t) = 1]$ is computed in the last elimination step before the MAP estimation, as in [4].

Finally, we compute quantities $d_{\mathcal{F}}(S; t)$ that are (approximately) proportional to joint probabilities $P[I_S(t) = 1]$. Due to this proportionality, $P[I_S(t) = 1]$ and $d_{\mathcal{F}}(S; t)$ are equivalent for the purpose of choosing a set that maximizes (3). The quantities $d_{\mathcal{F}}(S; t)$ are computed based only on time-of-day probabilities for single appliances and pairs of appliances (Section 2.1), using graph spectral representation. This way, only single and pairwise time-of-day probabilities ($P[I_S(t) = 1]$ for $S = \{a_i\}$ and $S = \{a_i, a_j\}$) need to be stored, and $d_{\mathcal{F}}(S; t)$ can be computed on the fly for any S.

To do this, we construct a graph of appliances and choose "distances" between pairs of appliances $\mathcal{F}$ as functions of their joint time-of-day probabilities. Specifically, for appliances a_i and a_j, we set a distance matrix $\mathbf{D}$

$$\mathbf{D}[i, j] = \mathbf{D}[j, i] = 1 - P[I_{\{a_i,a_j\}}(t) = 1], \quad (4)$$

so that large joint time-of-day probability means small distance. If there are any singleton sets ($S = \{a_k\}$) among the feasible sets in $\mathcal{F}$, then for each such appliance set we include a "dummy" appliance $a_{k'}$ in addition to appliance a_k with the following distances:

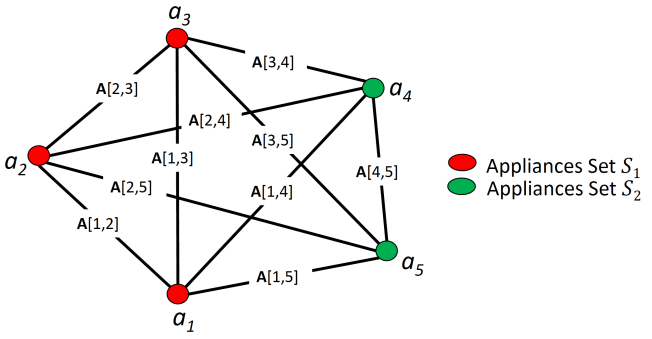

Fig. 2. Example of an appliance graph.

$$\mathbf{D}[k',j] = \mathbf{D}[j,k'] = \begin{cases} 1 - P[I_{\{a_k,a_j\}}(t) = 1], & \text{if } j \neq k \\ 1 - P[I_{\{a_k\}}(t) = 1], & \text{if } j = k \end{cases} \tag{5}$$

The affinity matrix $\mathbf{A}$ is obtained as

$$\mathbf{A}[i,j] = \exp\left\{-\frac{\mathbf{D}[i,j]}{2\sigma^2}\right\}, \tag{6}$$

where σ is set to the standard deviation of the values in $\mathbf{D}$, as in [16]. An example of an appliance graph is shown in Fig. 2, with affinities between appliances as edge weights. Next, the graph Laplacian matrix is computed as [17]:

$$\mathbf{L} = \mathbf{W}^{-1/2}\mathbf{A}\mathbf{W}^{-1/2}, \tag{7}$$

where $\mathbf{W}$ is a diagonal matrix whose entries are summations of the corresponding columns of $\mathbf{A}$. Then, eigenvectors $\mathbf{v}_1, \mathbf{v}_2, ..., \mathbf{v}_m$ corresponding to the m largest eigenvalues of $\mathbf{L}$ are used to construct a matrix $\mathbf{X} \in \mathbb{R}^{n \times m}$, as $\mathbf{X}[:,i] = \mathbf{v}_i$. Finally, the normalized i-th row of $\mathbf{X}$, $\mathbf{X}[i,:]$, represents appliance a_i as a vector in the $\mathbb{R}^m$ space [16, 17]. This is called spectral representation of the appliance graph.

The quantities $d_{\mathcal{F}}(S;t)$ are computed based on Euclidean distances of vectors $\mathbf{X}[i,:]$. Specifically, let N_j be the number of appliances in set $S_j \in \mathcal{F}$ and $\mathbf{c}_j$ be the centroid of the vectors representing those appliances:

$$\mathbf{c}_j = \frac{1}{N_j} \sum_{a_i \in S_j} \mathbf{X}[i,:]. \tag{8}$$

Then the average Euclidean distance AED_j of the vectors associated with S_j is

$$AED_j = \frac{1}{N_j} \sum_{a_i \in S_j} \|\mathbf{X}[i,:] - \mathbf{c}_j\|_2. \tag{9}$$

Finally, for each $S_j \in \mathcal{F}$, the quantity $d_{\mathcal{F}}(S_j;t)$ is computed as the normalized inverse AED_j:

$$d_{\mathcal{F}}(S_j;t) = \frac{\frac{1}{AED_j}}{\sum_{k=1}^{n_S} \frac{1}{AED_k}}. \tag{10}$$

These quantities are used in place of $P[I_S(t) = 1]$ in (3) for MAP estimation. Table 1 shows the feasible set $\mathcal{F}$ at two time instants t_1 and t_2 along with true probabilities $P[I_S(t) = 1]$ (computed from ground truth data) and quantities $d_{\mathcal{F}}(S;t)$ computed using the above approach. The data comes from the *tracebase* dataset [18]. As seen in the last column of the table, $d_{\mathcal{F}}(S;t)$ is approximately proportional to $P[I_S(t) = 1]$ at each time instant, albeit with different constants of proportionality at different times. This makes $d_{\mathcal{F}}(S;t)$ a good proxy for $P[I_S(t) = 1]$ when maximizing (3). Then after finding the turned ON set of appliance at time t, the mean power level of each appliance in this set is used as its disaggregated power level at time t.

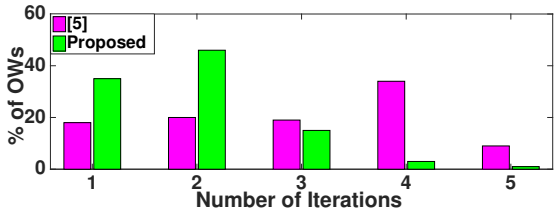

Fig. 3. Convergence speed improvement.

3. EXPERIMENTS

Two case studies are presented to demonstrate the effectiveness of the proposed NILM method. The accuracy of appliance state identification is evaluated using the well known F-score, as in [20], and the "Total Power Correctly Assigned (A_{cc})" metric [20] is used to evaluate the performance of power disaggregation. Further, in order to examine the appliance identification speed, the average execution time (denoted as AET) per OW is used (as described in [4]).

In the first case study, all six houses from the REDD dataset [21] and one house from the RAE dataset [22] were used. The REDD dataset consists of whole-home and circuit/appliance-specific active power measurements for six US houses over several months. All power measurements are at 3-second intervals. The first 26 days of data were used for the training phase, and the next 30 days were used to test the proposed method. The RAE dataset consists of whole-home and circuit/appliance-specific active power measurements for one Canadian house over 72 days. All power measurements are at 1-second intervals. The first 25 days of data were used for the training phase, and the next 38 days were used to test the proposed method.

Table 2 shows the average F-score, A_{cc} and AET over all houses in the REDD and RAE datasets for [4] and the proposed method. The average improvements in the F-score and A_{cc} are about 3.6% and 3.7%, respectively. This does not seem like much, but it is significant considering that [4] is already fairly accurate to start with (over 90%), so there is not much room to improve. The greatest benefit from the proposed method comes in reducing AET, which is decreased by over 40%, on average. Hence, incorporating joint statistics into appliance state identification, as proposed in Section 2.2, offers a significant speed up in convergence of the identification algorithm.

In order to further demonstrate the speed up, Fig. 3 shows the percentage of OWs in REDD House 1 where appliance

Table 1. True $P[I_{S_j}(t)=1]$ vs. $d_{\mathcal{F}}(S_j;t)$

Time t	Set $\mathcal{F}$	$P[I_{S_j}(t)=1]$	$d_{\mathcal{F}}(S_j;t)$	$\frac{P[I_{S_j}(t)=1]}{d_{\mathcal{F}}(S_j;t)]}$
t_1	$S_1 = \{$water kettle$\}$	0.383	0.371	1.032
	$S_2 = \{$toaster, iron$\}$	0.471	0.454	1.037
	$S_3 = \{$iron, lamp, projector$\}$	0.179	0.173	1.035
t_2	$S_1 = \{$cooking stove$\}$	0.732	0.587	1.245
	$S_2 = \{$toaster, lamp, desktop$\}$	0.511	0.413	1.240

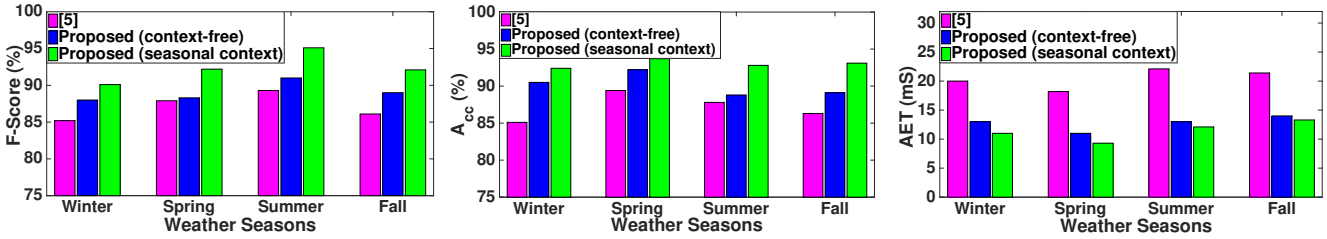

(a) F-score accuracy (b) A_{cc} accuracy (c) Average executions time

Fig. 4. Appliance identification results for the second case study using the AMPds2 dataset [19].

Table 2. Appliance identification results in the first case study using the REDD dataset [21] and REA dataset [22].

House Name	F-Score (%)		A_{cc} (%)		AET (ms)	
	[4]	Prop.	[4]	Prop.	[4]	Prop.
redd1	91.1	93.3	90.4	94.9	21.8	11.7
redd2	91.4	94.1	91.2	93.1	17.9	9.8
redd3	86.2	90.7	84.3	88.2	12.6	6.8
redd4	86.8	88.1	87.4	90.5	17.1	7.8
redd5	85.5	87.9	86.2	88.7	17.8	10.3
redd6	88.1	90.4	85.1	89.2	16.4	10.9
REA	86.8	91.3	87.9	90.5	19.8	11.4

identification converged in a given iteration. According to Fig. 3, the method in [4] had to execute 4 or 5 iterations in nearly 43% of OWs, while the proposed method converged in 3 iterations or less in 96% of OWs.

In the second case study, we evaluate the appliance state identification on the AMPds2 dataset [19]. This dataset contains whole-house and 21 circuit/appliance-specific active power power consumptions of a house in Canada over two years (from April 2012 to March 2014). All power measurements are at 1-minute intervals. We use the first year of appliance data for training and the second year of aggregated data for testing. Using the first year of data, we can generate time-of-day usage patterns over the whole year. We call these *context-free* patterns. In addition, since a full year of data is available for both training and testing, we also experimented with *seasonal context-based* patterns for four seasons (winter, spring, summer, and fall), where we use the resulting patterns in their corresponding seasonal context.

The average F-score, A_{cc} and the AET for appliance state identification in each season from April 2013 to March 2014 are presented in Figure 4(a), (b) and (c), respectively. Here, again, we compare the F-score, A_{cc} and AET against the method from [4]. For the proposed method, both the context-free and the seasonal context-based results are shown. As seen in the figures, the proposed context-free appliance state identification improves the F-score and A_{cc} slightly over [4], but also offers significant reduction in AET. The seasonal context-based appliance state identification offers further improvement in the F-score and A_{cc} and further reduction in AET, indicating that seasonal appliance usage patterns can be a useful piece of information for appliance state identification.

4. CONCLUSIONS

A improved NILM method was presented by utilizing time-of-day usage patterns of appliances. The appliance state identification make use of appliance graphs that enable efficient computation of time-of-day joint probabilities. This helps improve both the accuracy and speed of appliance state identification. Three publicly available datasets (REDD, RAE, AMPds2) were used to test the improved method. The results show the higher appliance identification accuracy and faster convergence of the algorithm. The proposed framework also allows for context-based appliance state identification and one such context, the current season, was examined. The results show that seasonal context helps further improve the accuracy and speed of appliance state identification.

In this paper, we used a considerable number of days (25 days for case study 1 and 365 days for case study 2) of individual appliance power profiles in a given house in order to obtain the corresponding time-of-day usage patterns. However, collecting this much data for the training phase is not practical in terms of hardware installation and the concerns of occupants. Therefore, in the future, we will investigate other methods to obtain time-of-day usage patterns with less training.

5. REFERENCES

[1] G. W. Hart, "Nonintrusive appliance load monitoring," *Proc. IEEE*, vol. 80, no. 12, pp. 1870–1891, Dec. 1992.

[2] S. Makonin, F. Popowich, I. V. Bajić, B. Gill, and L. Bartram, "Exploiting HMM sparsity to perform online real-time nonintrusive load monitoring," *IEEE Trans. Smart Grid*, vol. 7, no. 6, pp. 2575–2585, 2016.

[3] K. Basu, V. Debusschere, S. Bacha, U. Maulik, and S. Bondyopadhyay, "Non intrusive load monitoring: A temporal multi-label classification approach," *IEEE Trans. Ind. Informat.*, vol. 11, no. 4, pp. 689–698, 2015.

[4] C. Dinesh, B. W. Nettasinghe, R. I. Godaliyadda, M. P. B. Ekanayake, J. Ekanayake, and J. V. Wijayakulasooriya, "Residential appliance identification based on spectral information of low frequency smart meter measurements," *IEEE Trans. Smart Grid*, vol. 7, no. 6, pp. 2781–2792, Nov. 2016.

[5] C. Dinesh, P. H. Perera, G. M. R. I. Godaliyadda, M. P. B. Ekanayake, and J. B. Ekanayake, "Residential appliance monitoring based on low frequency smart meter measurements," in *IEEE International Conference on Smart Grid Communications (SmartGridComm)*, 2015, pp. 878–884.

[6] C. Dinesh, P. H. Perera, G. M. R. I. Godaliyadda, M. P. B. Ekanayake, and J. B. Ekanayake, "Individual power profile estimation of residential appliances using low frequency smart meter data," in *, IEEE International Conference on Industrial and Information Systems (ICIIS)*, 2015, pp. 140–145.

[7] C. Dinesh, R. I. Godaliyadda, M. P. B. Ekanayake, J. Ekanayake, and P. Perera, "Non-intrusive load monitoring based on low frequency active power measurements," *AIMS Energy*, vol. 4, no. 3, pp. 414–443, 2016.

[8] Stephen Makonin, Laura Guzman Flores, Robyn Gill, Roger Alex Clapp, Lyn Bartram, and Bob Gill, "A consumer bill of rights for energy conservation," in *Humanitarian Technology Conference-(IHTC), 2014 IEEE Canada International*. IEEE, 2014, pp. 1–6.

[9] Y. H. Lin and M. S. Tsai, "Development of an improved time frequency analysis-based nonintrusive load monitor for load demand identification," *IEEE Trans. Instrum. Meas.*, vol. 63, no. 6, pp. 1470–1483, 2014.

[10] M. Hazas, A. Friday, and J. Scott, "Look back before leaping forward: Four decades of domestic energy inquiry," *IEEE Pervasive Computing*, vol. 10, no. 1, pp. 13–19, 2011.

[11] T. Hassan, F. Javed, and N. Arshad, "An empirical investigation of V-I trajectory based load signatures for nonintrusive load monitoring," *IEEE Trans. Smart Grid*, vol. 5, no. 2, pp. 870–878, 2014.

[12] W. Wichakool, Z. Remscrim, U. A. Orji, and S. B. Leeb, "Smart metering of variable power loads," *IEEE Trans. Smart Grid*, vol. 6, no. 1, pp. 189–198, 2015.

[13] C. Dinesh, D. B. W. Nettasinghe, G. M. R. I. Godaliyadda, M. P. B. Ekanayake, J. V. Wijayakulasooriya, and J. B. Ekanayake, "A subspace signature based approach for residential appliances identification using less informative and low resolution smart meter data," in *2014 9th International Conference on Industrial and Information Systems (ICIIS)*, Dec 2014, pp. 1–6.

[14] O. Parson, S. Ghosh, M. Weal, and A. Rogers, "Nonintrusive load monitoring using prior models of general appliance types," in *AAAI-2012*, 2012.

[15] G. W. Hart, *Nonintrusive Appliance Load Data Acquisition Method: Progress Report*, MIT Energy Laboratory, 1984.

[16] W. M. Song, T. D. Matteo, and T. Aste, "Hierarchical information clustering by means of topologically embedded graphs," *PLoS One*, vol. 7, no. 3, pp. e31929, 2012.

[17] A. Ng, M. I. Jordan, and Y. Weiss, "On spectral clustering: Analysis and an algorithm," in *Proc. NIPS'02*, 2002, pp. 849–856.

[18] A. Reinhardt, P. Baumann, D. Burgstahler, M. Hollick, H. Chonov, M. Werner, and R. Steinmetz, "On the accuracy of appliance identification based on distributed load metering data," in *Proc. IEEE SustainIT*, Oct. 2012, pp. 1–9.

[19] S. Makonin, B. Ellert, I. Bajić, and F. Popowich, "Electricity, water, and natural gas consumption of a residential house in canada from 2012 to 2014," *Scientific Data*, vol. 3, pp. 1–12, 2016.

[20] S. Makonin and F. Popowich, "Nonintrusive load monitoring (NILM) performance evaluation," *Energy Efficiency*, vol. 8, no. 4, pp. 809–814, 2015.

[21] J. Kolter and M. Johnson, "REDD: a public data set for energy disaggregation research," in *Proc. ACM SustKDD*, 2011.

[22] S. Makonin, Z. J. Wang, and C. Tumpach, "RAE: The Rainforest Automation Energy Dataset for Smart Grid Meter Data Analysis," *arXiv preprint arXiv:1705.05767*, 2017.